Chapter 2
Pure Elastic Contact Force Models

Abstract The most important pure elastic constitutive laws commonly utilized to model and analyze contact-impact events in the context of multibody mechanical system dynamics are presented in this chapter. Additionally, the fundamental issues related to the generalized contact kinematics, developed under the framework of multibody system dynamics formulation, are briefly described. In this process, the main contact parameters are determined, namely the indentation or pseudo-penetration of the potential contacting points, and the normal contact velocity. Subsequently, the linear Hooke's contact force model and the nonlinear Hertz's law are presented together with a demonstrative example of application. Some other elastic contact force models are also briefly described.

Keywords Multibody dynamics · Contact kinematics · Elastic contact force models · Hooke force model · Hertz force model

2.1 Generalized Contact Kinematics

The generalized contact kinematics between two planar rigid bodies that can experience an oblique eccentric impact is first described. Figure 2.1a shows two convex bodies i and j in the state of separation that are moving with absolute velocities $\dot{\mathbf{r}}_i$ and $\dot{\mathbf{r}}_j$, respectively. The potential contact points are denoted by P_i and P_j (Machado et al. 2012).

The evaluation of the contact kinematics involves the calculation of three fundamental quantities, namely the position of the potential contact points, their Euclidian distance and their relative normal velocity (Glocker 2001; Machado et al. 2010). In general, this information must be available in order to allow the determination of the contact forces that develop during the contact-impact events (Lankarnai and Nikravesh 1990; Gilardi and Sharf 2002; Hippmann 2004; Askari et al. 2014). The possible motion of each body in a multibody system can be quantified in terms of the distance and relative velocity of the potential contact points. Positive values of that distance represent a separation, while negative values

P. Flores and H.M. Lankarani, *Contact Force Models for Multibody Dynamics*,
Solid Mechanics and Its Applications 226, DOI 10.1007/978-3-319-30897-5_2

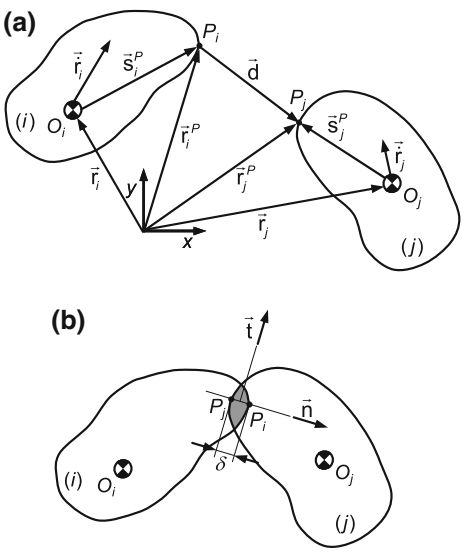

Fig. 2.1 **a** Two bodies in the state of separation; **b** two bodies in the state of contact (indentation, δ)

denote relative indentation or penetration of the contacting bodies. These two scenarios are illustrated in Fig. 2.1a, b, respectively. The change in sign of the normal distance indicates a transition from separation to contact, or vice versa (Flores and Ambrósio 2010). In turn, positive values of the relative normal velocity between the contact points, that is, the indentation or penetration velocity, indicate that the bodies are approaching, which corresponds to the "compression phase", while negative values denote that the bodies are separating, that corresponds to the "restitution phase". The vectors of interest in studying contact-impact events are represented in Fig. 2.1.

The vector that connects the two potential contact points, P_i and P_j, is a gap function that can be expressed as (Nikravesh 1988)

$$\mathbf{d} = \mathbf{r}_j^P - \mathbf{r}_i^P \tag{2.1}$$

where both $\mathbf{r}_i^P$ and $\mathbf{r}_j^P$ are described in global coordinates with respect to the inertial reference frame, that is

$$\mathbf{r}_k^P = \mathbf{r}_k + \mathbf{A}_i \mathbf{s}_i'^P \quad (k = i, j) \tag{2.2}$$

in which $\mathbf{r}_i$ and $\mathbf{r}_j$ represent the global position vectors of bodies i and j, while $\mathbf{s}_i'^P$ and $\mathbf{s}_j'^P$ are the local components of the contact points with respect to local coordinate systems. The planar rotational transformation matrices $\mathbf{A}_k$ are given by (Nikravesh 1988; Flores 2015)

$$\mathbf{A}_k = \begin{bmatrix} \cos\phi_k & -\sin\phi_k \\ \sin\phi_k & \cos\phi_k \end{bmatrix} \quad (k = i, j) \tag{2.3}$$

A normal vector to the plane of contact, illustrated in Fig. 2.1b, can be determined as

$$\mathbf{n} = \frac{\mathbf{d}}{d} \tag{2.4}$$

where the magnitude of the vector $\mathbf{d}$ is evaluated as

$$d = \mathbf{n}^T \mathbf{d} \tag{2.5}$$

The minimum distance condition given by Eq. (2.5) is not enough to find the possible contact points between the contact bodies, since it does not cover all possible scenarios that may occur in the contact problem. Therefore, the contact points are defined as those that correspond to maximum indentation, that is, the points of maximum relative deformation, measured along the normal direction (Lopes et al. 2010; Machado et al. 2014). Thus, three geometric conditions for contact can be defined as, (i) the distance between the potential contact points given by vector $\mathbf{d}$ corresponds to the minimum distance; (ii) the vector $\mathbf{d}$ has to be collinear with the normal vector $\mathbf{n}_i$; (iii) the normal vectors $\mathbf{n}_i$ and $\mathbf{n}_j$ at the potential contact points have to be collinear. The conditions (ii) and (iii) can be written as two cross products as (Machado et al. 2011)

$$\mathbf{n}_j \times \mathbf{n}_i = \mathbf{0} \tag{2.6}$$

$$\mathbf{d} \times \mathbf{n}_i = \mathbf{0} \tag{2.7}$$

The geometric conditions given by Eqs. (2.6) and (2.7) are two nonlinear equations with two unknowns, which can be solved using a Newton-Raphson iterative procedure (Atkinson 1989; Nikravesh 1988). This system of equations provides the solutions for the location of the potential contact points. Once the potential contact points are found, the next step deals with the evaluation of the relative indentation between the contact bodies as (Flores and Ambrósio 2004)

$$\delta = \sqrt{\mathbf{d}^T \mathbf{d}} \tag{2.8}$$

The velocities of the contact points expressed in terms of the global coordinate system are evaluated by differentiating Eq. (2.2) with respect to time, yielding

$$\dot{\mathbf{r}}_k^P = \dot{\mathbf{r}}_k + \dot{\mathbf{A}}_k \mathbf{s}_k'^P \quad (k = i, j) \tag{2.9}$$

in which the dot denotes the derivative with respect to time. The relative normal velocity is determined by projecting the contact velocity onto the direction normal to the plane of contact, yielding (Flores et al. 2004)

$$v_N = \dot{\delta} = \mathbf{n}^T \left(\dot{\mathbf{r}}_j^P - \dot{\mathbf{r}}_i^P \right) \tag{2.10}$$

This way of representing the relative normal velocity is quite convenient, in the measure that it is not necessary to deal with the derivation of the normal unit vector because this velocity component is not directly obtained by differentiating Eq. (2.5) (Flores et al. 2006; Tian et al. 2009). Furthermore, the fully rigid body velocity kinematics can easily be applied. The computational implementation of this methodology is quite efficient. However, the above description is restricted to convex rigid bodies with a smooth surface at least in a neighborhood of the potential contact points such that the contact area reduces to a single point which may move relative to the surfaces of the bodies. This approach can be extended to more generalized contact geometries as long as a common tangent plane of the contacting bodies is uniquely defined (Glocker 2004; Pombo and Ambrósio 2008; Machado et al. 2011, 2014).

2.2 Linear Hooke Contact Model

The simplest elastic contact force model is represented by a linear spring element, in which the spring embodies the elasticity of the contacting surfaces. This linear contact force model, also known as Hooke's law, can be expressed as (Shigley and Mischke 1989; Ravn 1998).

$$F_N = k\delta \tag{2.11}$$

where k is the spring stiffness and δ represents the relative penetration or deformation of the colliding bodies and F_N is the resulting normal contact force. The spring stiffness of the Hooke contact force model can be evaluated by using analytical expressions for simple cases, obtained by means of finite element method or determined through experimental tests performed within the linear elastic domain (Zhu et al. 1999; Machado et al. 2012; Koshy et al. 2013). In turn, the penetration is determined from the relative position of the contacting bodies.

One primary weakness associated with this contact force model is the quantification of the spring constant, which depends on the geometric and material characteristics of the contacting bodies. Furthermore, the assumption of a linear relation between the penetration and the contact force is at best a rough approximation, because the contact force is affected by the shape, surface conditions and mechanical properties of the contacting bodies, all of which suggest a more

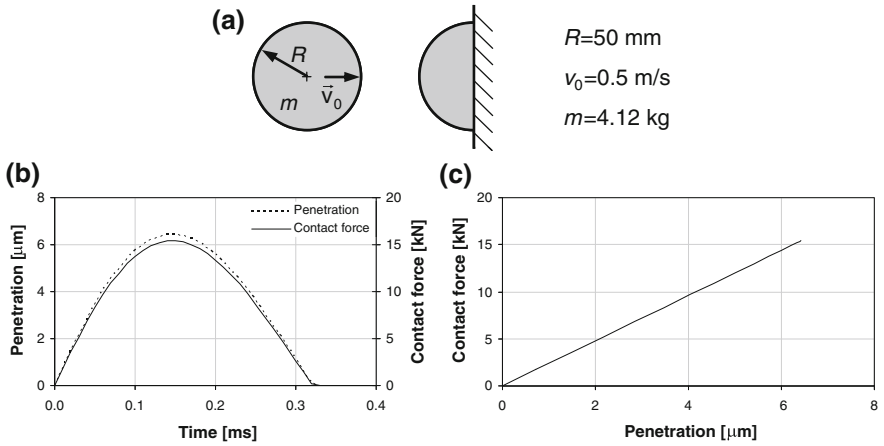

Fig. 2.2 Externally colliding spheres modeled by Hooke contact force law: **a** scenario of the impact between two spheres; **b** penetration and contact force versus time; **c** force-penetration relation

complex relation. In addition, the contact force model given by Eq. (2.11) does not account for the energy loss during an impact event.

For this linear contact force model, Fig. 2.2 shows the penetration δ, the normal contact force F_N and the force-penetration relation of two externally colliding spheres. The spheres are identical and have the same radius of 50 mm. The left sphere has an approaching initial velocity of 0.5 m/s, while the right sphere is stationary. A relative spring stiffness of 2.4×10^9 N/m is utilized for the results in Fig. 2.2. The spheres are considered to be made of steel with the Young's modulus and the Poisson's ratio of 207 GPa and 0.3, respectively.

2.3 Nonlinear Hertz Contact Model

The most popular contact force model for representing the collision between two spheres of isotropic materials is based on the work by Hertz, utilizing the theory of elasticity (Hertz 1881; Timoshenko and Goodier 1970; Flores et al. 2006). It should be noted that the Hertz contact theory is restricted to frictionless surfaces and perfectly elastic solids. The Hertz law relates the contact force with a nonlinear power function of penetration and is expressed as (Johnson 1982)

$$F_N = K\delta^n \tag{2.12}$$

where K is a generalized stiffness parameter and δ is the same relative penetration or indentation. The exponent n is equal to 3/2 for the case where there is a parabolic distribution of contact stresses, as in the original work by Hertz (1881). For

materials such as glass or polymer, the value of the exponent n can be either higher or lower, leading to a convenient contact force expression which is based on experimental work, but that should not be confused with the Hertz theory (Shivaswamy 1997; Ravn 1998; Dietl et al. 2000).

The generalized stiffness parameter K is dependent on the material properties and shape of the contact surfaces. For two spheres in contact, the generalized stiffness parameter is a function of radii of the spheres i and j and the material properties as (Goldsmith 1960)

$$K = \frac{4}{3(\sigma_i + \sigma_j)} \sqrt{\frac{R_i R_j}{R_i + R_j}} \tag{2.13}$$

in which the material parameters σ_i and σ_j are given by

$$\sigma_l = \frac{1 - \nu_l^2}{E_l}, \quad (l = i, j) \tag{2.14}$$

and the quantities ν_l and E_l are, respectively, the Poisson's ratio and Young's modulus associated with each sphere. For contact between a sphere i and a plane surface body j, the generalized stiffness parameter depends on the radius of the sphere and the material properties of the contacting surfaces, and is expressed as (Lankarani 1988; Flores et al. 2008)

$$K = \frac{4}{3(\sigma_i + \sigma_j)} \sqrt{R_i} \tag{2.15}$$

It is important to note that, by definition, the radius is negative for concave surfaces, such as in mechanical joint clearances, and positive for convex surfaces, such as in external impacts (Hertz 1881).

Figure 2.3 illustrates the penetration, the normal contact force and the force-penetration relation for two externally colliding spheres modeled by the Hertz

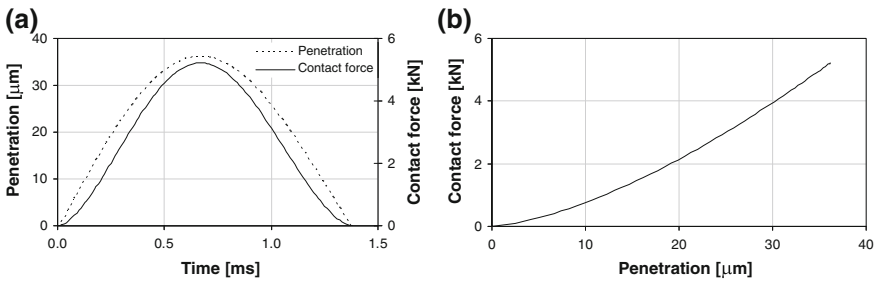

Fig. 2.3 Externally colliding spheres modeled by Hertz contact law: **a** penetration and contact force versus time; **b** force-penetration relation

contact force law. The generalized stiffness is evaluated for the two steel spheres to be 2.4×10^{10} N/m$^{3/2}$. The impact scenario is the same as described for the Hooke law example presented in Fig. 2.2. It is apparent that the Hertz contact law given by Eq. (2.12) is limited to contacts with elastic deformations and does not include energy dissipation. This contact force model represents the contact process as a non-linear spring along the direction of collision. The advantages of the Hertz model relative to Hooke law reside on its physical meaning represented by both its nonlinearity and by its relation between the generalized stiffness and geometric and material properties of the contacting surfaces. Although the Hertz law is based on the elasticity theory, several studies have been performed to extend its application to include energy dissipation. In fact, the process of energy transfer is an extremely complex task of modeling contact events. When an elastic body is subjected to cyclic loads, the energy loss due to internal damping causes a hysteresis loop in the force-penetration diagram, which corresponds to energy dissipation (Shivaswamy 1997; Alves et al. 2015).

2.4 Other Elastic Contact Models

Yang and Sun (1985) linearized the Hertz's law to model the contact force developed in spur gear dynamics, yielding the following expression

$$F_N = k\delta \tag{2.16}$$

in which the contact stiffness is given by

$$k = \frac{\pi EL}{4(1-\nu^2)} \tag{2.17}$$

where E is the Young's modulus, ν is the Poisson's ratio and L denotes the thickness of the gears. Dubowsky and Freudenstein (1971) also considered a linear relation between indentation and contact force for the case of contact of a journal inside of a bearing when the impact takes place at low velocity and the loads involved are small. The linearization of the Hertz's law may not be very accurate because it does not represent the overall nonlinear nature of an impact, and limits its application as it was avowed by Hunt and Crossley (1975).

One limitation associated with the Hertz's law deals with the evaluation of the contact stiffness parameter and nonlinear exponent, particularly when the bodies contact in a line or surface instead of a point (Pereira et al. 2011). For spherical contact geometries, where the contact areas assume a circular or ellipsoidal shape, the contact stiffness parameter used to define the constitutive contact force law is estimated by applying the Hertz theory of contact. However, for rectangular contact areas, that is, for contacts involving cylindrical shape bodies with parallel axis, the physical meaning of the contact stiffness parameter is not straightforward and its

value is not easy to obtain. In empirical and theoretical investigations, Brändlein et al. (1998) proposed the following mathematical relation for the contact between cylinders

$$F_N = K\delta^{1.08} \tag{2.18}$$

It is worth to note that K depends on the contact length and is independent of the contact radii of the bodies. A similar force-indentation relation for the contact between a cylinder of infinite length and a half space was presented by Nijen (1997).

Another weakness associated with Hertz's law is that it assumes that the size of contact area is small when compared to the curvature radii of the surfaces in contact. This assumption seems good enough for nonconformal contacts. However, for the case of conformal contacts this is not entirely true due to the large deformations that occur at the contact zone (Johnson 1999). Goodman and Keer (1965) demonstrated that conformal contacts can be up to 25 percent stiffer in compression than would be predicted by the Hertzian contact theory. This idea has been corroborated by Pereira et al. (2011). Liu et al. (2006) extended the Hertz contact law to propose a new force model for the particular case of spherical joints with clearance. In a previous work, Liu et al. (2005) presented a compliant force model for cylindrical joints with clearances, where the Hertz's law is only valid for large clearance sizes and small loads (Dubowsky and Freudenstein 1971; Tian et al. 2011). The force model proposed by Liu et al. (2005) can be expressed as

$$F_N = \frac{\pi E^* L \delta}{2}\left(\frac{\delta}{2(c+\delta)}\right)^{\frac{1}{2}} \tag{2.19}$$

where E^* represents the composite modulus of the two colliding cylinders, L is the length of cylindrical joint, δ denotes the relative indentation and c is the radial clearance size. This approach was compared and validated with results obtained with FEM analysis (Liu et al. 2007). The composite modulus can be evaluated using the following mathematical expression

$$E^* = \left(\frac{1-\nu_i^2}{E_i} + \frac{1-\nu_j^2}{E_j}\right)^{-1} \tag{2.20}$$

More recently, Luo and Nahon (2011) extended the Hertz contact approach for polyhedral contacting bodies, namely for line and face contacting objects, in which they explicitly consider the distinction between true contact geometry and interference geometry. This new approach was accompanied with both FEM and experimental discussions. Another way to overcome the difficulties of the Hertz's law, when the contact area cannot be represented as a single contact point, is to consider the elastic foundation approach (Hippmann 2004). This model is based on representation of the body surfaces by polygon meshes and contact force

determination by the elastic foundation model. This approach allows for the modeling of contact between complex geometries and scenarios where the contact area is relatively large, having good computational efficiency when compared with the FEM analysis. Bei and Fregly (2004) proposed a computationally efficient methodology for combining multibody dynamic simulation method with a deformable contact knee model. In this study, the contact between knee surfaces was modeled through the use of the elastic foundation approach for both natural and artificial knee articulations. Pérez-González et al. (2008) developed a modified elastic foundation approach for application in three-dimensional models of the prosthetic knees, in which both contacting bodies are considered to be deformable solids with their own elastic properties. Mukras et al. (2010) also used the elastic foundation method to evaluate the contact forces for wear modeling and analysis in the framework of multibody systems formulations. Their results obtained for a planar slider-crank mechanism with a dry clearance revolute joint were compared and validated with those produced via FEM.

At this stage, it must be noted that the contact force models described in this chapter do not consider the energy dissipation during the contact process. In fact, the process of energy transfer is an extremely complex task of modeling contact-impact events. When a body is subjected to cyclic loads, the energy loss due to internal damping causes a hysteresis loop in the force-indentation diagram, which corresponds to energy dissipation. Krempf and Sabot (1993) identified the damping capability of a dry sphere pressed against a plate made by steel (Hertzian contact) from experimental nonlinear resonance curves. These authors observed that the contact damping shows approximately viscous behavior (Kelvin and Voigt like). This corresponds to the theoretical considerations presented by Hunt and Crossley (1975). Sabot et al. (1998) experimentally studied a ball normally preloaded by a moving rigid mass. They clearly exhibited the softening primary resonance when no loss of contact occurs and analyzed mechanical sources of damping. In a similar manner to Krempf and Sabot, Johnson (1961) measured the energy loss within a dry contact, in which two spherical surfaces were pressed together and excited by an oscillating force. The force direction deviates from the normal direction to the contact plane, and notable energy dissipation was observed. The fundamental issues associated with internal damping that occurs in the contact process will be analyzed and discussed in the next chapter.

References

Alves J, Peixinho N, Silva MT, Flores P, Lankarani HM (2015) A comparative study of the viscoelastic constitutive models for frictionless contact interfaces in solids. Mech Mach Theory 85:172–188

Askari E, Flores P, Dabirrahmani D, Appleyard R (2014) Study of the friction-induced vibration and contact mechanics of artificial hip joints. Tribol Int 70:1–10

Atkinson KA (1989) An introduction to numerical analysis, 2nd edn. Wiley, New York

Bei Y, Fregly BJ (2004) Multibody dynamic simulation of knee contact mechanics. Med Eng Phys 26:777–789

Brändlein J, Eschamann P, Hasbargen L (1998) Die Wälzlagerpraxis. Handbuch für die Berechnung und Gestaltung von Lagerungen. Vereinigte Fachverlage, Germany

Dietl P, Wensing J, van Nijen GC (2000) Rolling bearing damping for dynamic analysis of multi-body systems—experimental and theoretical results. Proc Inst Mech Eng Part K J Multibody Dyn 214(1):33–43

Dubowsky S, Freudenstein F (1971) Dynamic analysis of mechanical systems with clearances, Part 1: Formulation of dynamic model. J Eng Ind 93:305–309

Flores P (2015) Concepts and Formulations for Spatial Multibody Dynamics. Springer, Berlin

Flores P, Ambrósio J (2004) Revolute joints with clearance in multibody systems. Comput Struct 82:359–1369

Flores P, Ambrósio J (2010) On the contact detection for contact-impact analysis in multibody systems. Multibody Syst Dyn 24(1):103–122

Flores P, Ambrósio J, Claro JCP, Lankarani HM (2006) Influence of the contact-impact force model on the dynamic response of multibody systems. Proc Inst Mech Eng Part K J Multibody Dyn 220(1):21–34

Flores P, Ambrósio J, Claro JCP, Lankarani HM (2008) Translational joints with clearance in rigid multi-body systems. J Comput Nonlinear Dyn 3:0110071–10

Flores P, Ambrósio J, Claro JP (2004) Dynamic analysis for planar multibody mechanical systems with lubricated joints. Multibody Syst Dyn 12(1):47–74

Gilardi G, Sharf I (2002) Literature survey of contact dynamics modeling. Mech Mach Theory 37:1213–1239

Glocker C (2001) On frictionless impact models in rigid-body systems. Philos Trans Math Phys Eng Sci 359:2385–2404

Glocker C (2004) Concepts for modeling impacts without friction. Acta Mech 168:1–19

Goldsmith W (1960) Impact—the theory and physical behaviour of colliding solids. Edward Arnold Ltd, London, England

Goodman LE, Keer LM (1965) The contact stress problem for an elastic sphere indenting an elastic cavity. Int J Solids Struct 1:407–415

Hertz H (1881) Über die Berührung fester elastischer Körper. J reine und angewandte Mathematik 92:156–171

Hippmann G (2004) An algorithm for compliant contact between complexly shaped bodies. Multibody Syst Dyn 12:345–362

Hunt KH, Crossley FRE (1975) Coefficient of restitution interpreted as damping in vibroimpact. J Appl Mech 7:440–445

Johnson KL (1961) Energy dissipation at spherical surfaces in contact transmitting oscillating forces. J Mech Eng Sci 3:362–368

Johnson KL (1982) One hundred years of Hertz contact. Proc Inst Mech Eng 196:363–378

Johnson KL (1999) Contact mechanics. Cambridge University Press, Cambridge

Koshy CS, Flores P, Lankarani HM (2013) Study of the effect of contact force model on the dynamic response of mechanical systems with dry clearance joints: computational and experimental approaches. Nonlinear Dyn 73(1–2):325–338

Krempf P, Sabot J (1993) Identification of the damping in a Hertzian contact from experimental non-linear response curve. In: Proceedings of the IUTAM symposium on identification of mechanical systems. University of Wuppertal, Germany

Lankarani HM (1988) Canonical equations of motion and estimation of parameters in the analysis of impact problems. PhD Dissertation, University of Arizona, Tucson, Arizona, USA

Lankarani HM, Nikravesh PE (1990) A contact force model with hysteresis damping for impact analysis of multibody systems. J Mech Des 112:369–376

Liu C, Zhang K, Yang L (2005) The compliance contact model of cylindrical joints with clearances. Acta Mech Sin 21:451–458

Liu C, Zhang K, Yang L (2006) Normal force-displacement relationship of spherical joints with clearances. J Comput Nonlinear Dyn 1:160–167

Liu C, Zhang K, Yang R (2007) The FEM analysis and approximate model for cylindrical joints with clearances. Mech Mach Theory 42:183–197

Lopes DS, Silva MT, Ambrósio JA, Flores P (2010) A mathematical framework for rigid contact detection between quadric and superquadric surfaces. Multibody Syst Dyn 24(3):255–280

Luo L, Nahon M (2011) Development and validation of geometry-based compliant contact models. J Comput Nonlinear Dyn 6:0110041–11

Machado M, Flores P, Ambrósio J (2014) A lookup-table-based approach for spatial analysis of contact problems. J Comput Nonlinear Dyn 9(4):041010

Machado M, Flores P, Ambrósio J, Completo A (2011) Influence of the contact model on the dynamic response of the human knee joint. Proc Inst Mech Eng Part K J Multibody Dyn 225 (4):344–358

Machado M, Flores P, Claro JCP, Ambrósio J, Silva M, Completo A, Lankarani HM (2010) Development of a planar multi-body model of the human knee joint. Nonlinear Dyn 60:459–478

Machado M, Moreira P, Flores P, Lankarani HM (2012) Compliant contact force models in multibody dynamics: evolution of the Hertz contact theory. Mech Mach Theory 53:99–121

Mukras S, Mauntler A, Kim NH, Schmitz TL, Sawyer WG (2010) Evaluation of contact force and elastic foundation models for wear analysis of multibody systems. In: Proceedings of the ASME 2010 international design engineering technology conferences. Montreal, Quebec, Canada, Paper No: DETC2010-28750, 15–18 Aug

Nijen G (1997) On the overrolling of local imperfections in rolling bearings. Ph.D. Dissertation, University of Twente, The Netherlands

Nikravesh PE (1988) Computer-aided analysis of mechanical systems. Prentice Hall, Englewood Cliffs, New Jersey

Pereira CM, Ramalho AL, Jmbrósio JA (2011) A critical overview of internal and external cylinder contact force models. Nonlinear Dyn 63:681–697

Pérez-González A, Fenollosa-Esteve C, Sancho-Bru JL, Sánchez-Marín FT, Vergara M, Rodríguez-Cervantes PJ (2008) A modified elastic foundation contact model for application in 3D models of the prosthetic knee. Med Eng Phys 30(3):387–398

Pombo J, Ambrósio J (2008) Application of a wheel-rail contact model to railway dynamics in small radius curved tracks. Multibody Syst Dyn 19(1–2):91–114

Ravn P (1998) A continuous analysis method for planar multibody systems with joint clearance. Multibody Syst Dyn 2:1–24

Sabot J, Krempf P, Janolin C (1998) Nonlinear vibrations of a sphere-plane contact excited by a normal load. J Sound Vib 214:359–375

Shigley JE, Mischke CR (1989) Mechanical engineering design. McGraw-Hill, New York

Shivaswamy S (1997) Modeling contact forces and energy dissipation during impact in multibody mechanical systems. Ph.D. Dissertation, Wichita State University, Wichita, Kansas, USA

Tian Q, Liu C, Machado M, Flores P (2011) A new model for dry and lubricated cylindrical joints with clearance in spatial flexible multibody systems. Nonlinear Dyn 64:25–47

Tian Q, Zhang Y, Chen L, Flores P (2009) Dynamics of spatial flexible multibody systems with clearance and lubricated spherical joints. Comput Struct 87(13–14):913–929

Timoshenko SP, Goodier JN (1970) Theory of elasticity. McGraw Hill, New York

Yang DCH, Sun ZS (1985) A rotary model for spur gear dynamics. J Mech Transmissions Autom Des 107:529–535

Zhu SH, Zwiebel S, Bernhardt G (1999) Theoretical formula for calculating damping in the impact of two bodies in a multibody system. Proc Inst Mech Eng, Part C J Mech Eng Sci 213:211–216

Springer

http://www.springer.com/978-3-319-30896-8

Contact Force Models for Multibody Dynamics

Flores, P.; Lankarani, H.M.

2016, VIII, 171 p. 94 illus., 3 illus. in color., Hardcover
ISBN: 978-3-319-30896-8